Pergamon

Int. J. Heat Mass Transfer. Vol. 39, No. 9, pp. 1993–2003, 1996

0017-9310/96 $15.00+0.00

0017-9310(95)00296-0

Performance and optimum dimensions of different cooling fins with a temperature-dependent heat transfer coefficient

K. LAOR and H. KALMAN†

Pearlstone Center for Aeronautical Engineering Studies, Department of Mechanical Engineering, Ben-Gurion University of the Negev, Beer Sheva 84105, Israel

(*Received in final form* 14 *March* 1995)

Abstract—This paper presents a theoretical-numerical analysis of longitudinal and annular fins and spines. We examine rectangular, triangular and parabolic profiles for the fins and cylindrical, conical and parabolic spines. In order to reach an understanding of the performance of these odd-shaped, but real world fins, the situation examined here is the case of fins subject to a temperature-dependent heat transfer coefficient. Figures as well as numerical correlations of performance and optimum dimensions of these fins are presented.

INTRODUCTION

Fins are a widely used device in the augmentation of heat transfer and play an important role in thermal systems design. Therefore, optimized fins have long been the desire of the designer. 'Real world' analysis can be very complex. Many investigators have adopted and analyzed fins using the idealizing assumptions that are attributed to Murray [1] and Gardner [2]:

(1) the heat flow and temperature distribution throughout the fin are independent of time, i.e. the heat flow is steady;

(2) the fin material is homogeneous and isotropic;

(3) there are no heat sources in the fin itself;

(4) the heat flow to or from the fin surface at any point is directly proportional to the temperature difference between the surface at that point and the surrounding fluid;

(5) the thermal conductivity of the fin is constant;

(6) the heat-transfer coefficient is the same all over the fin surface;

(7) the temperature of the surrounding fluid is uniform;

(8) the temperature of the base of the fin is uniform;

(9) the fin thickness is so small compared to its height that temperature gradients normal to the surface may be neglected;

(10) the heat transfer through the outermost edge of the fin is negligible compared to that which passes through the sides.

Hung and Appl [3], Aziz [4] and Jang and Bejan [5] assumed the thermal conductivity to be linearly dependent on the temperature excess of the fin surfaces over the surroundings. Brown [6], Irey [7], Lau and Tan [8], Laor and Kalman [9], Laor [35], Maday [10] and Ünal [11] considered also the heat dissipation from the fin tip and the heat transfer coefficient was assumed to be constant over the fin surface, or temperature dependent [10, 11]. Irey [7], Levitsky [12] and Lau and Tan [8] examined the criterion and errors due to one-dimensional heat transfer analysis and concluded that the fin base thickness Biot number should be much smaller than unity. Snider and Kraus [13] confirmed this conclusion by taking into account the tapered fin effect.

Ghai and Jakob [14] and Ghai [15] experimentally demonstrated that heat transfer coefficients attained significantly greater values at the fin tip rather than at the fin base and concluded that the idealization of a uniform heat transfer coefficient is not necessarily realistic. Since then, papers analyzing the coordinate dependent heat convection fins have been published and many of these reports have been reviewed by Huang and Shah [16]. Razelos and Imre [17, 18] assumed that the heat transfer coefficient varies according to a power law of the distance from the base. They found the optimum dimensions of circular and longitudinal fins but not those of spines. Their approach may result in exact solutions for measured local heat transfer coefficients, but cannot be applied to a design of finned systems. In any case, the known heat convection mechanism is mostly temperature dependent. Obviously, each mechanism for any kind of fin eventually results in a heat transfer coefficient that is location dependent.

In certain applications, the heat loss may vary with the local temperature in a nonlinear manner. In particular, the cooling process may be governed by a power law-type temperature dependence. Under these

† Author to whom correspondence should be addressed.

NOMENCLATURE

a heat convection definition, equation (2)
A_n cross-section area, normal to the heat flow direction [m^2]
B, C, D, E, J, U variables which distinguish between different fins, Table 2
Bi_s Biot number based on length, $2h_0 s/k$
F shape factor
g gravitational acceleration [$m\ s^{-2}$]
G volume integration, equation (9)
Gr Grashof number, $g\beta(T\text{-}T_\infty)s^3/v^2$
h heat transfer coefficient [$W\ m^{-2}\ °C^{-1}$]
H_1, H_2, K_1, K_2 correlation parameters, equations (11)–(13), Table 3
k thermal conductivity [$W\ m^{-1}\ °C^{-1}$]
L sharp ended fin length [m]
L_f cut fin length [m]
M fin mass [kg]
m power of convection coefficient
m_f fin parameter, $L\sqrt{(2h_0)/(k\,\delta_0)}$
n constant for fin shape definition (0, 1 or 2)
P fin perimeter [m] or pressure [$N\ m^{-2}$]
Pr Prandtl number, v/α
q heat rate, [W]
q/A heat flux [$W\ m^{-2}$]
R_0 annular fin base radius [m]
s characterizing length [m]
S active surface area of the fin [m^2]
T temperature [°C]
T_∞ temperature of surroundings [°C]
x distance from the fin base [m]
Z longitudinal fin width [m].

Greek letters

α thermal diffusivity [$m^2\ s^{-1}$]
β volumetric coefficient of expansion [K^{-1}]
δ fin thickness [m]
ε emissivity
η fin efficiency
θ temperature excess of fin over surroundings [°C]
v kinematic viscosity [$m^2\ s^{-1}$]
ρ material's density [$kg\ m^{-3}$]
σ Stefan–Boltzmann constant, $5.669 \cdot 10^{-8}$ [$W\ m^{-2}\ K^{-4}$]
ϕ normalized temperature $= \theta/\theta_0$.

Subscripts

0 fin base
f film temperature.

circumstances, the differential equation for temperature becomes strictly nonlinear [19]. Ünal [20] analyzed one-dimensional longitudinal fins having a rectangular profile, assuming that the heat transfer coefficient is a power function of the difference between the temperature of the fin and that of the ambient fluids. Sen and Trinh [19] further derived the rate of heat dissipation for the same fin.

For longitudinal fins, the optimization problem has been solved by Schmidt [21] and confirmed by Duffin [22] and Duffin and McLain [23]. In order to find the fin profile they assumed that the minimum weight fin has a linear temperature distribution along its length. This approach has been adopted by Cobble [24], Maday [10] and Jang and Bejan [5] for straight fins and by Guceri and Maday [25] and Mikk [26] for annular fins, with and without assuming the length of arc. The resulting fin shapes are complex and have little practical use, mainly due to manufacturing problems. Kern and Kraus [32] used a different approach in which they calculated the optimum dimensions for known shapes of different types of fins. The same approach was used by Brown [6], Ullmann and Kalman [27] and Kalman and Tavi [28] for annular fins.

Cobble [21] derived the optimum dimensions of a straight fin that exchanges heat with the surroundings by a constant convection coefficient and radiation. Cash *et al.* [29] examined the optimum fin for boiling heat transfer. There are no publications regarding optimization of fins with a temperature dependent heat transfer coefficient nor for variable fin shapes. Optimization of such fins is of great importance for understanding optimum fins with known mechanisms of heat exchange with the surroundings.

In this study, longitudinal, spine and annular fins each with rectangular, triangular and parabolic shapes, governed by power law-type temperature dependence of the heat transfer coefficient, have been examined. The governing equation was solved numerically by a recognized technique [9], [27], [28], [30] and [35]. The efficiency, optimum dimensions and performance have been shown graphically to correlate to simple equations that achieve quick and accurate design. Although practical application involves other effects such as temperature dependency of thermal conductivity of fin material, two-dimensional heat flow, and so on, only the heat transfer coefficient effect is considered. This is in order to reach an effective presentation of the results. However, we take into account structural considerations that have been studied elsewhere [9, 28 and 35].

TEMPERATURE DISTRIBUTION

The convection heat transfer coefficient, h, is usually assumed to be constant for the analysis of cooling fins, but, in reality, it is temperature or location dependent. In either laminar or turbulent forced convection, the heat transfer coefficient is a function of location. For plates (longitudinal fins), the local heat transfer coefficient depends on the location along the flow path. For cylinders (spines), the local heat transfer coefficient depends on the location on the periphery. In this study, the heat balance will be defined as one-dimensional and as a function of the axis along the heat conduction flow which is perpendicular to the axis of the local heat transfer coefficient variation. Therefore, we cover forced convection by applying the average heat transfer coefficient, assuming negligible heat conduction within the fin perpendicular to the main conduction direction along the fin. In free convection, the local heat transfer coefficient is location and temperature dependent.

For fins used in free convection, the location dependence is in the gravity direction which is usually perpendicular to the main heat conductivity flow along the fin. As for forced convection, this location-dependency is averaged and only the temperature-dependency is maintained. The averaged Nusselt number can be represented in the following functional form for a variety of isothermal circumstances [33]:

$$\bar{N}u_f = c(Gr_f Pr_f)^m, \tag{1}$$

where the subscript f indicates that the properties are evaluated at the film temperature. It is clear from equation (1) that the heat transfer coefficient is only temperature dependent, and can be written as follows:

$$h = a\theta^m. \tag{2}$$

Equation (2) is suitable for heat transfer coefficients in free convection from isothermal surfaces as well as free convection from constant heat flux surfaces. It is also suitable for forced convection by applying $m = 0$. Equation (2) is also suitable for boiling from different surfaces and space radiation (zero ambient temperature). Considering the heat transfer coefficient at the base temperature, $h_0 = a\theta_0^m$, equation (2) is redefined

$$h = h_0\phi^m, \tag{3}$$

where values of h_0 and m from simplified equations [33] are shown in Table 1, for free convection to air, boiling to water, and radiation. For free convection $m = 1/3$ or $1/4$, for radiation $m = 3$ and for boiling $m = 1/7$, $1/3$, 2 or 3. For a constant heat transfer coefficient, $m = 0$, can be used. Although different cases have the same m power, they differ by the value of h_0. All the cases described in Table 1 can be treated with $m = 1/7$, $1/4$, $1/3$, 2 and 3, while h_0 remains a free parameter. Notice that the heat transfer coefficient for horizontal cylinders (spines) at laminar free convection is diameter dependent (Table 1). The diameter is decreasing along the conical and parabolic spines. This significantly affects the heat transfer coefficient. In this study, only temperature dependent heat transfer coefficients are considered, therefore the following analyses and figures are not relevant for such cases.

Heat balance on a differential length of any type of fin (longitudinal, spine or annular) with any shape (rectangular, triangular or parabolic) is shown in Fig. 1. Using the same approach as that shown previously by Kalman and co-workers (including the length of arc), yields

$$\frac{d}{dx}\left(-kA_n\frac{dT}{dx}\right)+hP\left[\frac{1}{4}\left(\frac{d\delta}{dx}\right)^2+1\right]^{1/2}(T-T_\infty)=0, \tag{4}$$

where x starts at the fin base and is normal to it, P and A_n are the fin perimeter and the fin area normal to the heat flow, respectively, at distance x from the fin base.

Introducing the definitions of P and A_n from Table 2 and their derivatives, the non-dimensional variables are $\bar{A} = A_n/A_{n0}$, $\bar{\delta} = \delta/\delta_0$, $\bar{x} = x/L$, $\phi = (T-T_\infty)/(T_0-T_\infty)$. Inserting equation (3) into equation (4) results in a general second-order differential equation

$$\frac{d^2\phi}{d\bar{x}^2}-B\frac{d\phi}{d\bar{x}}-C\frac{m_f^2}{(1-\bar{x})^n}\times\left[\frac{n^2(1-\bar{x})^{2n-2}}{4}\left(\frac{\delta_0}{L}\right)^2+1\right]^{1/2}\phi^{m+1}=0, \tag{5}$$

where the fin parameter $m_f = L\sqrt{(2h_0)/(k\delta_0)}$, L is the fin length and the three shapes are defined by a single equation

$$\bar{\delta} = \frac{\delta}{\delta_0} = (1-\bar{x})^n, \tag{6}$$

where n represents the fin shape. Although n may be a real number defining complicated shapes, only three values for n ($n = 0$ for rectangular fins, $n = 1$ for triangular fins and $n = 2$ for parabolic fins) are considered in this paper. Nevertheless, performance of fin shapes represented by n values between 0 and 2 can be estimated from the following figures. Parameters B and C are defined separately for each type of fin in Table 2, and δ_0 is the fin thickness at the base. Equation (5) is suitable for heat transfer coefficients defined in equation (2). Problems involving mixed mechanisms such as free with forced convection, convection with radiation and forced convection with boiling, can be solved by the same procedure, only parameter C is a temperature function [31, 34]. Combined mechanisms are beyond the scope of this study mainly because they present too many possibilities.

Table 1. Values of h_0 and m for different heat transfer mechanisms (Holman [33])

Mechanism	Condition	h_0	m
Free convection	*Vertical plate or cylinder*		
	laminar $10^4 < GrPr < 10^9$	$1.42\left(\frac{\theta_0}{L}\right)^{1/4}$	1/4
	turbulent $GrPr > 10^9$	$1.31\theta_0^{1/3}$	1/3
	Horizontal cylinder		
	laminar $10^4 < GrPr < 10^9$	$1.32\left(\frac{\theta_0}{\delta}\right)^{1/4}$	1/4
	turbulent $GrPr > 10^9$	$1.24\theta_0^{1/3}$	1/3
	Horizontal plate—various conditions	$1.32\left(\frac{\theta_0}{L}\right)^{1/4}$	1/4
		$1.52\theta_0^{1/3}$	1/3
		$0.59\left(\frac{\theta_0}{L}\right)^{1/4}$	1/4
Fully developed boiling	$0.2 < P < 0.7$ MPa	$2.253\theta_0^3$	3
	$0.7 < P < 14$ MPa	$283.2P^{4/3}\theta_0^2$	2
	Horizontal plate		
	$q/A < 16$	$1042\theta_0^{1/3}$	1/3
	$16 < q/A < 240$	$5.56\theta_0^3$	3
	Vertical plate		
	$q/A < 3$	$537\theta_0^{1/7}$	1/7
	$3 < q/A < 63$	$7.96\theta_0^3$	3
Radiation	$T_\infty = 0$	$\sigma\varepsilon F\theta_0^3$	3

The second-order differential equation (5) is solved by using two boundary conditions

$$\phi_{\bar{x}=0} = 1$$

$$\left.\frac{d\phi}{d\bar{x}}\right|_{\bar{x}=\bar{L}_f} = -Bi_L\phi^{m+1}, \tag{7}$$

where $Bi_L = h_0L/k$, and $\bar{L}_f$ is the normalized distance of the fin tip from its base. $\bar{L}_f$ can have values between 0 and 1, while $\bar{L}_f = 1$ represents sharp ended triangular and parabolic fins and any other value represents cut fins. Although the effect of cutting sharp ended fins is not analyzed in this study (it has been previously studied by Kalman and Tavi [28] for annular fins with a constant heat transfer coefficient) it was kept in the equations in order to maintain generality. The second boundary condition represents heat dissipation from the fin tip [9, 35] and can be altered by insulation, hence $d\phi/d\bar{x} = 0$ at $\bar{x} = \bar{L}_f$.

Considering $\bar{x}$ as the only independent variable and keeping the other variables constant, equation (5) is solved numerically for all cases. A known technique for solving a two-point boundary value problem was used. It assumes first $d\phi/d\bar{x}$ at $\bar{x} = 0$ and then it checks if the second boundary condition is satisfied; if not, the assumption is corrected and the procedure is repeated.

Figure 2 presents the temperature distribution of the constant thickness longitudinal fin with an insulated tip for two values of the fin parameter and for four convection mechanisms. The numerical solutions show higher temperatures along the fin for higher values of m. This phenomenon can be misunderstood if one assumes that m is the only parameter defining the heat transfer mechanism. The convection mechanism is governed also by h_0 and furthermore, it also affects m_f.

The numerical solution is confirmed by the ana-

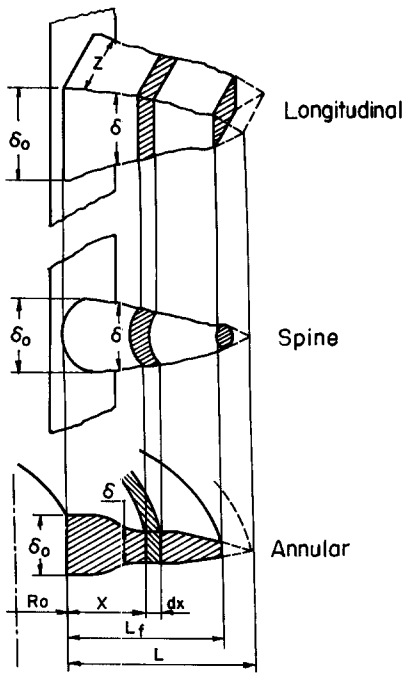

Fig. 1. Control volume for heat balance.

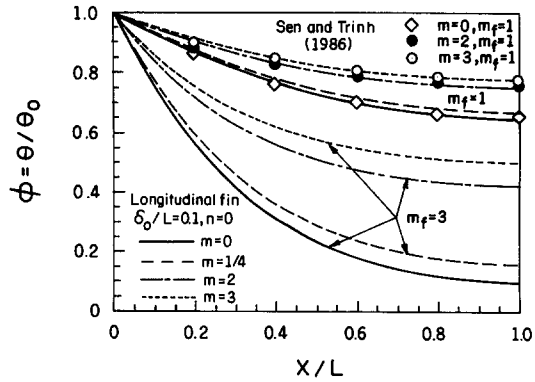

Fig. 2. Temperature distribution of constant thickness longitudinal fin of tip insulated for four convection mechanisms.

lytical solution of Sen and Trinh [17] for $m_f = 1$. It is clear from Fig. 2 that the temperature decrease is more moderate for higher values of the convection coefficient's power m. The slope of the temperature profile is steeper as m decreases, thus more heat is dissipated by the fin.

FIN EFFICIENCY

Fin efficiency is defined as the ratio between the heat removed by the fin and the heat that would have been removed if the entire surface area of the fin had been maintained at the base temperature.

$$\eta = q_f/q_{f0}. \tag{8}$$

By knowing the temperature profile from the solution of equation (5) and by applying Fourier's law at the fin base, the amount of heat that enters the fin and is transferred to the environment can be calculated, as

$$q_f = -\frac{kA_{n0}\theta_0}{L}\left.\frac{d\phi}{d\bar{x}}\right|_{\bar{x}=0}. \tag{9}$$

If the surface temperature of the fin is constant at the base temperature, calculating the heat that is dissipated from the fin is reduced to the calculation of the surface area by applying Newton's law of convection

$$q_{f0} = hS\theta_0, \tag{10}$$

where the surface area, S is

Table 2. Parameters expressions

Fin	Longitudinal	Spine	Annular
P	$2(Z+\delta)$	$\pi\delta$	$4\pi(R_0+x)$
$\bar{A}_n$	$(1-\bar{x})^n$	$(1-\bar{x})^{2n}$	$\left(1+\frac{\bar{x}}{\bar{R}_0}\right)(1-\bar{x})^n$
B	$\frac{n}{1-\bar{x}}$	$2\frac{n}{1-\bar{x}}$	$\frac{n}{1-\bar{x}}-\frac{1}{\bar{R}_0-\bar{x}}$
C	$1+(1-\bar{x})^n\frac{\delta_0}{Z}$	2	1
D	$1+(1-\bar{x})^n\frac{\delta_0}{Z}$	$2(1-\bar{x})^n$	$1+\frac{\bar{x}}{R_0}$
E	$(1-\bar{L}_f)^n$	$(1-\bar{L}_f)^{2n}$	$\left(1+\frac{\bar{L}_f}{\bar{R}_0}\right)(1-\bar{L}_f)^n$
J	1	2	1
U	0	0	$\frac{1}{\bar{R}_0}$

$$S = \int_0^{\bar{L}_f} PL\left[\frac{1}{4}\left(\frac{\mathrm{d}\bar{\delta}}{\mathrm{d}\bar{x}}\right)^2\left(\frac{\delta_0}{L}\right)^2 + 1\right]^{1/2} \mathrm{d}\bar{x} + A_n(\bar{L}_f). \quad (11)$$

Introducing the derivative of equation (6) into equation (11), substituting the perimeter and base area from Table 2 into equations (9) and (11), and then introducing equations (9)–(11) into the efficiency definition (8) yields the following expression of fin efficiency:

$$\eta = -\frac{1}{m_f^2}\frac{\left.\frac{\mathrm{d}\phi}{\mathrm{d}\bar{x}}\right|_{\bar{x}=0}}{\int_0^{\bar{L}_f} D\left[\frac{n^2(1-\bar{x})^{2n-2}}{4}\left(\frac{\delta_0}{L}\right)^2 + 1\right]^{1/2}\mathrm{d}\bar{x} + \frac{1}{2}\left(\frac{\delta_0}{L}\right)E}. \quad (12)$$

The second term of the denominator (due to the tip boundary condition) vanishes for the insulated tip ($E = 0$). For convicting tips, D and E are defined separately for each fin type in Table 2.

The integral solution for any fin is important for calculating the heat flux based on fin efficiency. The integral solution can be found in mathematical handbooks or can be solved numerically for more complex cases. It follows from equation (12) that the temperature distribution or, at least, the first derivative of the temperature at the fin base, enables fin efficiency to be defined for known shapes. Notice, however, that for any kind of rectangular fin, the efficiency and temperature profile do not depend on δ_0/L.

The equations for temperature distribution as well as for the efficiency derived in this study are general, and therefore valid for the three most common types of fins (longitudinal, spine and annular) and for the three most common cross-section shapes (rectangular, triangular and parabolic). The sharp ended fins—triangular and parabolic—can be cut at any length from the fin base by assigning $\bar{L}_f$ values between 0 and 1 (for safety). The slope of the fin surface is determined by δ_0 and L, but the real end of the fin is determined by L_f.

The numerical results of fin efficiency for the three fin shapes of idealized ($m = 0$) longitudinal fins and spines against the fin parameter, m_f are shown in Fig. 3. The numerical solutions of annular fins are presented elsewhere [28]. Figure 3 is identical to the analytical solutions of Gardner [2] and Kern and Kraus [32]. Fin efficiency is obviously at its maximum when fin length is zero. As the fin parameter increases, fin efficiency decreases, first slightly (for $m_f < 0.2$), then sharply, and stabilizes at large fin parameters. δ_0/L influences fin efficiency no more than does the line thickness on Fig. 3 for values from 0.01 to 0.5, which on further examination leads to the conclusion that δ_0/L has little effect on efficiency. Nevertheless the exact value used for calculations is indicated in the following figures even though the solution can be extrapolated to any practical value.

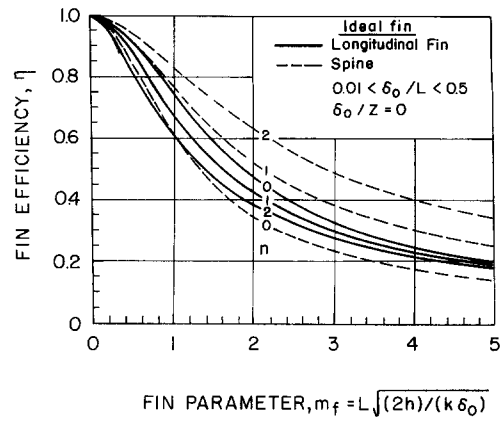

Fig. 3. The efficiency of ideal longitudinal fins and spines ($m = 0$ and insulated tip).

The difference between the efficiency of various shapes is greater for spines represented in Fig. 3, due to several reasons. The absolute value of the temperature gradient at the base [the numerator in equation (12)] as well as the surface area [the denominator in equation (12)] of both longitudinal fins and spines increases with increasing shape parameter, n. For a large width, Z, of the longitudinal fin, the increase of the surface area is much less than that of spines. This means that the shape parameter has less effect on the efficiency of longitudinal fins than it does on the efficiency of spines.

Fin efficiency against fin parameter are plotted for longitudinal fins, spines and annular fins with temperature dependent heat transfer coefficients in Figs. 4–6, respectively. The general behavior of fin efficiency is much the same for each type of fin, shape or heat convection power. Nevertheless, efficiency is higher for each defined fin parameter as heat convection power decreases; thus, more heat is dissipated from the base to the surroundings. These figures enable the designer to calculate heat dissipation. The behavior for $m = 1/7$ is not shown, but it obviously lies between the solutions of $m = 0$ and $m = 1/4$, and can be estimated from them.

FIN OPTIMIZATION

Fin optimizations can be achieved in either one of two ways: by maximizing the heat dissipation from the fin for any constant mass or volume, or by minimizing the volume for any given heat dissipation. In this paper the first method is used.

The heat dissipation from the fin surface to the surroundings can be found by applying the temperature distribution, $\phi(x)$ in equation (5), into Fourier's law of heat conduction. Assuming constant den-

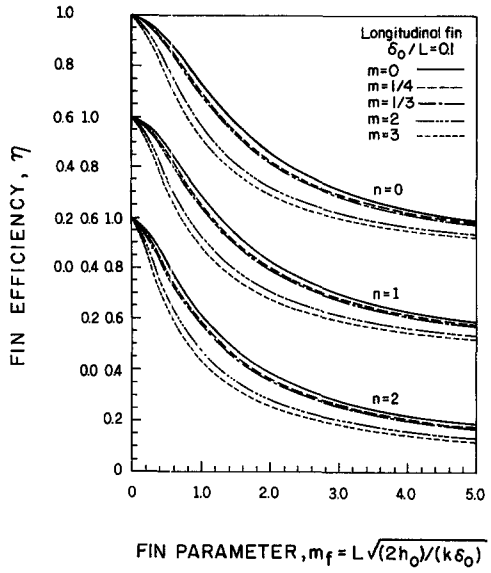

Fig. 4. Efficiency of longitudinal fins.

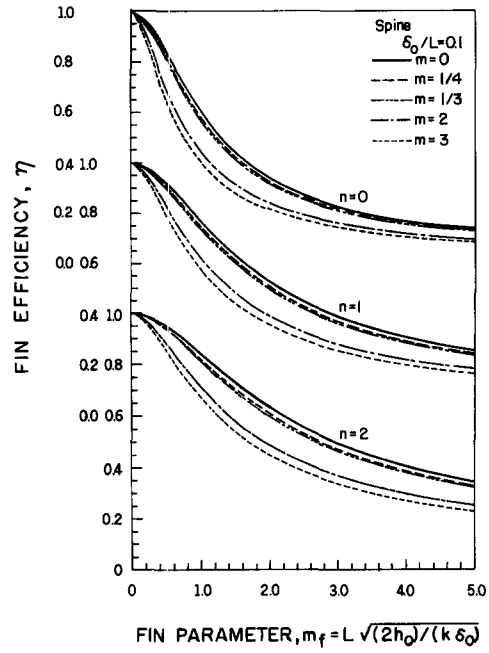

Fig. 5. Efficiency of spines.

sity of the fin material, the mass of the fin is obtained by its volume

$$M = \rho V = \rho \cdot \int_0^{L_f} A_n \, dx = \rho A_{n0} L \cdot G, \qquad (13)$$

where A_{n0} is the fin base area and G represents the result of the above integration

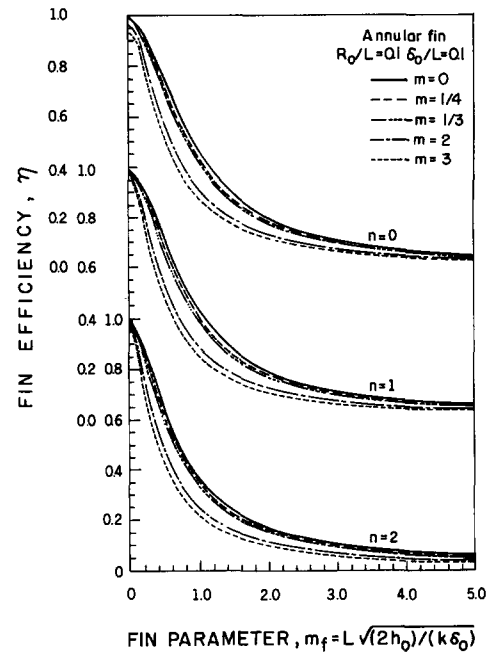

Fig. 6. Efficiency of annular fins.

$$G = \sum_{i=0}^{J\cdot n} \frac{\bar{x}(1-\bar{x})^i}{J\cdot n+1}\left[1+\frac{(i+1)\bar{x}}{n+2}U\right] \qquad (14)$$

where J and U are defined in Table 2 for each type of fin.

Using Fourier's law and equation (5), the heat per mass is defined as

$$\frac{q}{M} = -\frac{k(T_0-T_\infty)}{\rho}\frac{1}{L^2}\frac{1}{G}\frac{d\phi}{d\bar{x}}\bigg|_{\bar{x}=0}. \qquad (15)$$

The heat per mass is plotted in Fig. 7 vs L for longitudinal fins with constant heat transfer coefficient and insulated tip, as an example of the optimization procedure. It is essential to keep this preliminary figure in its dimensional form in order to emphasize the physical behavior and optimization procedure. Sometimes, normalization in the early stages of the study can be misleading and basic phenomena overlooked. Obviously, from Fig. 7, there is a maximum value of heat dissipation per mass for any fin volume and condition. Similar figures can be shown for spines and annular fins [28]. The dimensions of the different fins in which this maximum occurs are attributed to the optimum fin. By examining this figure, it can be concluded that for larger volumes (mass) the optimum fin is longer and dissipates more heat, although the heat dissipation per mass is lower.

The lines that describe the optimum dimensions and heat per mass can be found by an accumulation of the maximum values for slight and continuous increase of the volume. Let heat dissipation be normalized by $hb^2(T_0-T_\infty)$ and fin mass by ρb^3, where b is a

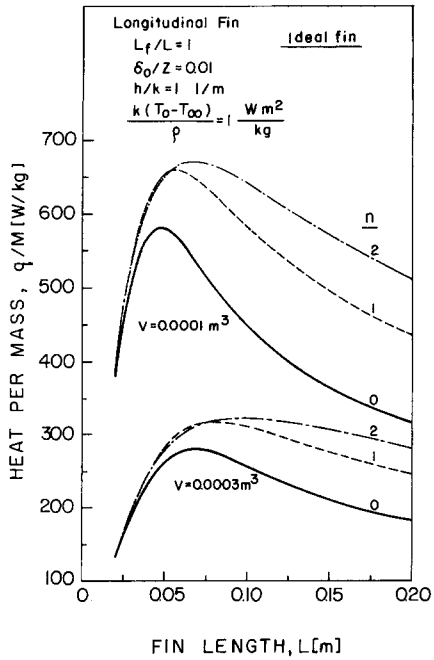

Fig. 7. Heat dissipation per mass of longitudinal fin and constant heat transfer coefficient ($m = 0$ and insulated tip).

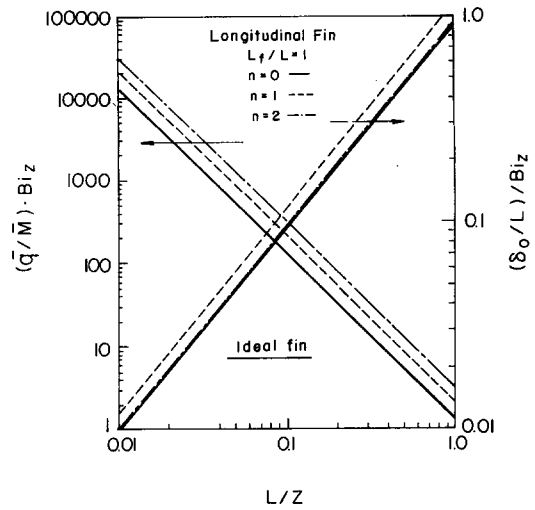

Fig. 8. The optimized heat dissipation per mass and dimensions for longitudinal fins with constant heat transfer coefficient and insulated tip.

characteristic length of the base. Then the dimensionless heat dissipation per mass is defined as follows:

$$\frac{\bar{q}}{\bar{M}} = -\frac{1}{Bi_L}\frac{b}{L}\frac{1}{G}\frac{d\phi}{d\bar{x}}\bigg|_{\bar{x}=0}. \tag{16}$$

By using $b = R_0$ for annular fins it has been shown [28] that $(\bar{q}/\bar{M})\cdot Bi_{R_0}$ and $(\delta_0/L)/Bi_{R_0}$ vs L/R_0, using logarithmic scales, appear to be linear. This enables the development of a single correlation for the optimized fin heat per mass and dimensions

$$\frac{\bar{q}}{\bar{M}} = \frac{K_1}{Bi_{R_0}}\left(\frac{L}{Z}\right)^{H_1}; \quad \frac{\delta_0}{L} = K_2 Bi_{R_0}\left(\frac{L}{Z}\right)^{H_2}. \tag{17}$$

By applying $b = Z$ for longitudinal fins with $m = 0$, the same phenomena can be seen in Fig. 8, although this figure is plotted for a unit length width, namely $Z = 1$ m. Therefore, for longitudinal fins also, a single correlation can describe the optimized fin heat per mass and dimensions

$$\frac{\bar{q}}{\bar{M}} = \frac{K_1}{Bi_Z}\left(\frac{L}{Z}\right)^{H_1} \quad \frac{\delta_0}{L} = K_2 Bi_Z\left(\frac{L}{Z}\right)^{H_2}. \tag{18}$$

For spines, the only base length is δ_0 which is not a free parameter as is R_0 for annular fins or unit width for longitudinal fins. Therefore, normalization of the length is impossible, but if one is forced (for uniformity) to use equation (16) for $b = \delta_0$ then $(\bar{q}/\bar{M})\cdot(Bi_{\delta_0}/\delta_0^2)$ and $(\delta_0/L)\cdot(\delta_0/Bi_{\delta_0})$ are plotted vs L in Fig. 9 to reach the same linearity and uniqueness of the two previous fins. It should be noted, however, that Fig. 9 is not dimensionless, but single correlations can be defined

$$\frac{\bar{q}}{\bar{M}} = K_1\frac{\delta_0^2}{Bi_{\delta_0}}L^{H_1} \quad \frac{\delta_0}{L} = K_2\frac{Bi_{\delta_0}}{\delta_0}L^{H_2}. \tag{19}$$

Optimum dimensions, as well as normalized heat per mass of constant thickness fins with variable heat

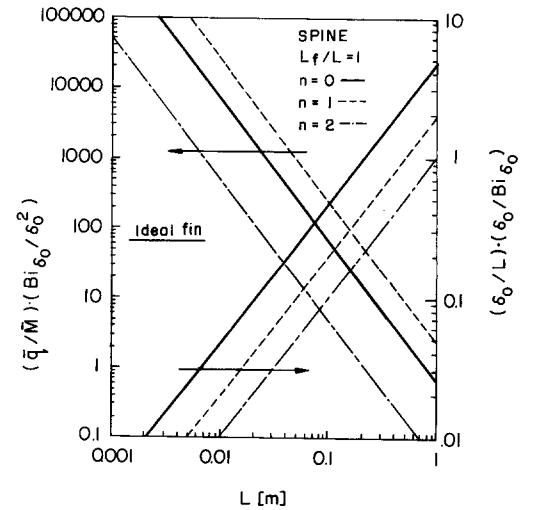

Fig. 9. The optimized heat dissipation per mass and dimensions for spines with constant heat transfer coefficient and insulated tip.

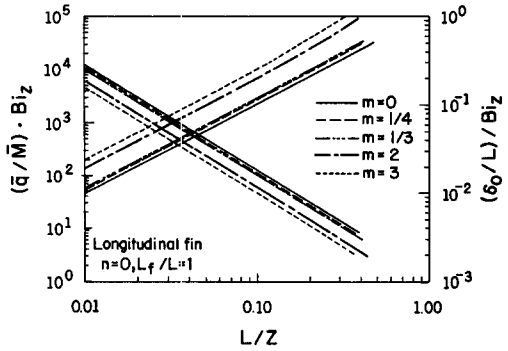

Fig. 10. Optimum behavior of constant thickness longitudinal fins.

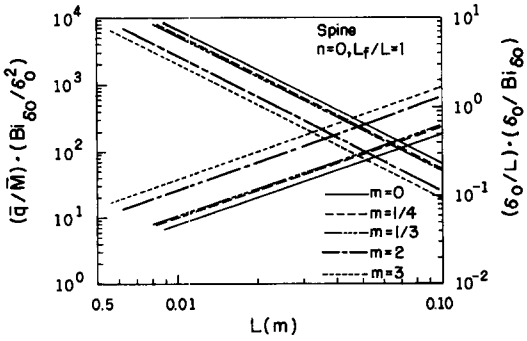

Fig. 11. Optimum behavior of constant thickness spines.

transfer coefficients, are shown in Figs. 10–12 for longitudinal, spine and annular fins, respectively. As fin length increases, normalized heat per mass decreases and base thickness increases. It is also obvious from these figures that normalized heat per mass increases for any fin length as the convection power, m, decreases. The values of correlation parameters H_1, K_1, H_2 and K_2 are presented in Table 3 for constant thickness (as in Figs. 10–12) as well as for triangular and parabolic shapes for the three types of fins. An analytic solution for the optimized dimensions of ideal longitudinal fins can be found in Kern and Kraus [32]. Their parameter values are listed in Table 3 and are reasonably close to the numeric values of this study.

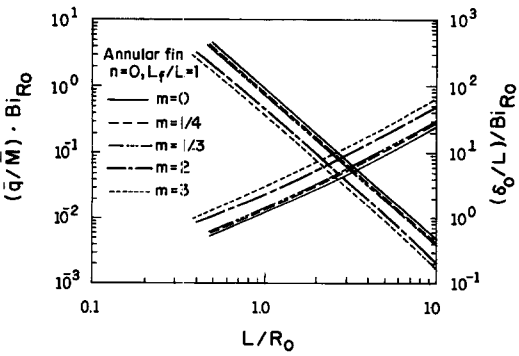

Fig. 12. Optimum behavior of constant thickness annular fins.

Using the correlations (17)–(19) enables the designer to consider 'real' optimum fins from any point of view. The simplest example would be a problem in which the length, L, is given. In this case the base thickness, δ_0, as well as the heat dissipation can be easily calculated for each fin type, shape, material and convection mechanism. Otherwise, trial and error should be used in order to calculate the same parameters. In any case, the fin shape, material and convection mechanism can be varied in order to choose the best ones, taking into account material, manufacturing and other costs.

CONCLUSIONS

In this study we defined unique equations for temperature distribution, efficiency, optimum dimensions and heat per mass. The uniqueness of these equations is their generality and applicability to three types of fins with three possible shapes. The equations in this study have been solved numerically by a method that was confirmed by comparison of ideal fin solutions to known analytical solutions.

The method presented in this paper made it possible to analyze the effect of the temperature dependent heat convection coefficient on performance and optimum dimensions. Longitudinal fins, spines and annular fins with rectangular, triangular and parabolic shapes, subject to various heat transfer coefficients corresponding to free convection, boiling and radiation were analyzed. The efficiency of each fin was presented graphically. The optimum fin performance as well as the dimensions were also presented graphically for some cases, and by simple correlations for all cases.

The variety of cases leading to 'real fins' are too wide to include in a general survey. Nevertheless, the same procedure can be applied to any location-dependent heat transfer coefficient as well as to mixed mechanisms and other effects. Mixed mechanism problems can be estimated by superposition of each separate mechanism. Adding, for example, the heat dissipation (calculated by efficiency) of one mechanism to the heat dissipation of another, would probably be more accurate than using available solutions for constant heat transfer coefficients. The ability to consider location and temperature dependent heat transfer coefficients for single fins would lead to further theoretical analysis and optimization of both fin arrays and fin surface compact heat exchangers. In these cases the

Table 3. Correlation parameters

Fin	m	H_1	K_1	H_2	K_2
Longitudinal	Ideal fin	−2.000	1.292	1.000	0.973
$n = 0$	[32]			1.000	0.990
	0	−2.006	1.255	1.012	1.027
	1/4	−2.008	1.100	1.014	1.149
	1/3	−2.009	1.055	1.016	1.192
	2	−2.022	0.563	1.040	2.211
	3	−2.026	0.435	1.047	2.883
Longitudinal	[32]			1.000	1.170
$n = 1$	0	−1.999	2.090	1.000	1.144
	1/4	−2.000	1.868	1.000	1.246
	1/3	−2.000	1.805	1.001	1.282
	2	−2.000	1.052	1.001	2.052
	3	−2.001	0.835	1.002	2.546
Longitudinal	[32]			1.000	1.000
$n = 2$	0	−2.000	3.053	1.000	0.994
	1/4	−2.000	2.746	1.000	1.079
	1/3	−2.000	2.649	1.001	1.111
	2	−2.000	1.566	1.001	1.766
	3	−2.000	1.252	1.001	2.177
Spine	Ideal fin	−2.000	0.683	1.000	4.640
$n = 0$	0	−2.036	0.592	1.054	5.742
	1/4	−2.044	0.484	1.065	7.085
	1/3	−2.047	0.455	1.069	7.575
	2	−2.049	0.220	1.075	15.852
	3	−1.967	0.245	1.000	14.067
Spine	0	−2.000	2.420	1.000	1.934
$n = 1$	1/4	−2.002	2.060	1.003	2.257
	1/3	−2.002	1.968	1.002	2.358
	2	−2.005	1.002	1.007	4.566
	3	−2.009	0.765	1.012	5.982
Spine	0	−2.055	0.038	1.014	1.032
$n = 2$	2	−2.003	0.022	1.004	2.268
	3	−2.005	0.017	1.007	2.946
Annular	Ideal fin	−2.299	0.940	1.263	1.250
$n = 0$	0	−2.169	0.958	1.136	1.350
	1/4	−2.336	0.855	1.350	1.349
	1/3	−2.336	0.825	1.360	1.360
	2	−2.350	0.462	1.410	2.249
	3	−2.349	0.362	1.410	2.858
Annular	0	−2.089	0.014	1.116	19.943
$n = 1$	1/4	−2.088	0.012	1.114	21.483
	1/3	−2.088	0.012	1.113	22.017
	2	−2.000	1.096	1.001	2.063
	3	−2.001	0.873	1.002	2.552
Annular	0	−2.093	0.020	1.149	19.977
$n = 2$	1/4	−2.089	0.018	1.143	21.111
	1/3	−2.089	0.017	1.142	21.580
	2	−2.081	0.011	1.126	32.036
	3	−2.081	0.009	1.125	39.140

heat transfer coefficient depends also on the distance between fins.

REFERENCES

1. W. M. Murray, Heat dissipation through an annular disk or fin of uniform thickness, *J. Appl. Mech.* **5:A78** (1938).
2. K. A. Gardner, Efficiency of extended surface, *Trans. ASME* **67,** 621–631 (1945).
3. H. M. Hung and F. C. Appl, Heat transfer of thin fins with temperature-dependent thermal properties and internal heat generation, *ASME J. Heat Transfer* **89,** 155–162 (1967).
4. A. Aziz, Perturbation solution for convective fin with internal heat generation and temperature dependent thermal conductivity, *Int. J. Heat Mass Transfer* **20,** 1253–1255 (1977).
5. P. Jang and A. Bejam, Ernst Schmidt's approach to fin optimization: an extension to fins with variable conductivity and the design of ducts for fluid flow, *Int. J. Heat Mass Transfer* **8,** 1635–1644 (1988).
6. A. Brown, Optimum dimensions of uniform annular fins, *Int. J. Heat Mass Transfer* **8,** 655–662 (1965).
7. R. K. Irey, Errors in the one-dimensional fin solution, *ASME J. Heat Transfer* **90,** 175–176 (1968).
8. W. Lau and C. W. Tan, Errors in one-dimensional heat transfer analysis in straight and annular fins, *ASME J. Heat Transfer* **95,** 549–551 (1973).
9. K. Laor and H. Kalman, The effect of tip convection on the performance and optimum dimensions of cooling fins, *Int. Commun. Heat Mass Transfer* **19,** 569–584 (1992).
10. C. J. Maday, The minimum weight one-dimensional straight cooling fin, *J. Engng Ind.* **96,** 161–165 (1974).
11. H. C. Ünal, The effect of the boundary condition at a fin tip on the performance of the fin with and without internal heat generation, *Int. J. Heat Mass Transfer* **31,** 1483–1496 (1988).
12. M. Levitsky, The criterion for validity for the fin approximation, *Int. J. Heat Mass Transfer* **15,** 1960–1963 (1972).
13. A. D. Snider and A. D. Kraus, Recent developments in the analysis and design of extended surfaces, *ASME J. Heat Transfer* **105,** 302–306 (1983).
14. M. L. Ghai and M. Jakob, Local coefficients of heat transfer on fins, ASME Paper 50-5-18 (1950).
15. M. L. Ghai, Heat transfer in straight fins, *Proceedings of General Discussion on Heat Transfer*, pp. 203–204. Institution of Mechanical Engineers, London (1951).
16. L. J. Huang and R. K. Shah, Assessment of calculation methods for efficiency of straight fins of rectangular profile, *ASME HTO*, Vol. 182, *Advances in Heat Exchanger Design, Radiation and Combustion*, pp. 19–30 (1991).
17. P. Razelos and K. Imre, The optimum dimensions of circular fins with variable thermal parameters, *ASME J. Heat Transfer* **102,** 420–425 (1980).
18. P. Razelos and K. Imre, Minimum mass convective fins with variable heat transfer coefficients, *J. Franklin Inst.* **315,** 269–282 (1980).
19. A. K. Sen and S. Trinh, An exact solution for the rate of heat transfer from a rectangular fin governed by a power law-type temperature dependence, *ASME J. Heat Transfer* **108,** 457–459 (1986).
20. H. C. Ünal, Determination of the temperature distribution in an extended surface with a non-uniform heat transfer coefficient, *Int. J. Heat Mass Transfer* **28,** 2279–2284 (1985).
21. E. Schmidt, Die wärmeübertragung durch rippen, *Z. Ver. Dt. Ing.* **70,** 885–951 (1926).
22. R. J. Duffin, A variational problem relating to cooling fins, *J. Math. Mech.* **8,** 47–56 (1959).
23. R. J. Duffin and D. K. McLain, Optimum shape of a cooling fin on a convex cylinder, *J. Math. Mech.* **17,** 769–784 (1968).
24. M. H. Cobble, Optimum fin shape, *J. Franklin Inst.* **291,** 283–292 (1971).
25. S. Guceri and C. J. Maday, A least weight circular cooling fin, *J. Engng Ind.* **97,** 1190–1193 (1975).
26. I. Mikk, Convective fin of minimum mass, *Int. J. Heat Mass Transfer* **23,** 707–711 (1980).
27. A. Ullmann and H. Kalman, Efficiency and optimized dimensions of annular fins of different cross-section shapes, *Int. J. Heat Mass Transfer* **32,** 1105–1110 (1989).
28. H. Kalman and M. Tavi, The effect of cutting sharp-ended annular fins on the efficiency and optimized dimensions, *Proceedings of the 9th International Heat Transfer Conference*, Vol. 4, pp. 3–7. Hemisphere, Washington, DC (1990).
29. D. R. Cash, G. J. Klein and J. W. Westwater, Approximate optimum fin design for boiling heat transfer, *ASME J. Heat Transfer* **93,** 19–24 (1971).
30. K. Laor and H. Kalman, Performance and temperature distributions in different fins with uniform and non-uniform heat generation, *Proceedings of the 1st European Thermal-Science and 3rd UK National Heat Transfer Conference*, Vol. 1, pp. 335–342. Hemisphere, London (1992).
31. E. Assis and H. Kalman, Transient temperature response of different fins to step initial conditions, *Int. J. Heat Mass Transfer* **36,** 4107–4114 (1993).
32. D. Q. Kern and A. D. Kraus, *Extended Surface Heat Transfer* (1st Edn). McGraw-Hill, New York (1972).
33. J. P. Holman, *Heat Transfer* (SI Metric Edn). McGraw-Hill, New York (1989).
34. E. Assis, K. Laor and H. Kalman, Experimental and theoretical investigation of the transient temperature response of spines in free convection, *Exp. Therm. Fluid Sci.* **9,** 289–298 (1994).
35. K. Laor, Performance and optimization of cooling fins, M. Sc. thesis, Ben-Gurion University of the Negev, Beer Sheva, Israel (1993).